Kinetic Simulations of Ion Beam Neutralization

O. Chang and J. Wang

Astronautical Engineering Department
University of Southern California
Los Angeles, CA 90089-1192, USA

Abstract. Full particle PIC simulations are performed to study the neutralization of an ion beam in the cohesionless, mesothermal regime. Simulations further confirmed that neutralization is achieved through interactions between the trapped electrons and the potential well established by the propagation of the beam front along the beam direction and is not through plasma instabilities as previous studies suggested. In the transverse direction, the process is similar to that of the expansion of mesothermal plasma into vacuum. Parametric simulations are also performed to investigate the effects of beam radius and domain boundary condition on the neutralization process. The results suggests that, while the qualitative behavior may be similar in ground tests, quantitative parameters such as the beam potential will be affected significantly by the vacuum chamber because of the limits imposed on the expansion process by the finite chamber space.

Keywords: Plasma Kinetic Theory, Particle-In-Cell, Electric Propulsion
PACS: 52.20-j, 51.10+y, 94.05.-a

INTRODUCTION

Ion beam emission/neutralization is one of the most fundamental problems in electric propulsion. It is well known that, in order to transmit a current exceeding the space charge limit from spacecraft to the ambient, the beam must be adequately neutralized or the transmission would be blocked by virtual anode formation in the beam [1] and spacecraft charging. Hence, the operation of an electric thruster or any other large current ion emitting source from spacecraft requires a neutralizer to neutralize the ion beam. In such systems, the ions are typically emitted as a cold beam while the electrons are typically emitted as stationary thermal electrons from the neutralizer. The emission is such that $v_{te} \gg v_{beam} \gg v_{ti}$, where v_{te}, v_{beam}, v_{ti} are the electron thermal velocity, beam drifting velocity, and ion thermal velocity, respectively, and the electron current emitted equals the ion current emitted. One notes that the plasma emitted is strongly non-neutral near the source regardless of the neutralizer location or the emitting surface area. Even for a hypothetical situation where the electrons and ions were emitted from exactly the same location and same surface area, the initial beam would still be strongly non-neutral due to the difference in electron and ion emitting velocity.

The ion beam neutralization process not only is an interesting physics problem but also has important practical implications. For instance, such knowledge is important in the neutralization design for electric thruster clusters. It is obviously also of critical importance in any modeling studies involving plasma emission. Ion beam neutralization is one of the first problems studied during electric propulsion development. Although ion beam neutralization is readily achieved in experiments, the understanding of the underlying physical process remains at a rather primitive level. No theoretical or simulation models have convincingly explained the detailed neutralization mechanism.

Earlier theoretical and simulations models have considered the neutralization of infinitively large uniform ion beam [2, 3, 4, 5, 6]. More recent models have considered a more realistic setting for finite size ion beam emission [7, 8, 9]. These previous studies suggest that wave-particle interaction and plasma instability may be the driving neutralization mechanism. However, no conclusions have been reached. Part of the reason for the lack of a good understanding of the neutralization process is because particle simulation of beam neutralization is an extremely challenging problem due to computational constraints. This is because, in order to simulate the physics correctly, such simulations must be carried out using the realistic ion to electron mass ratio so the correct mesothermal velocity order for ions and electrons, $v_{te} \gg v_{beam} \gg v_{ti}$ can be maintained. Additionally one must also use a very large simulation domain in order to minimize the effects of the simulation domain boundary.

Recently, Wang and Usui [10] studied the dynamic process of the emission and neutralization of a mesothermal plasma beam using full particle PIC simulation. They find that beam neutralization and propagation are two closely coupled processes. The initial expansion of thermal electrons over cold beam ions establishes an ion-acoustic-like beam front along the propagation direction. Subsequently, the emitted electrons are trapped in the region between the

forward propagating beam front and the emitting source. Electron-ion coupling is achieved through the interactions between the trapped electrons and the potential well along the beam direction. Beam neutralization is not through plasma instabilities as previous studies suggested. Self-similar expansion of ion acoustic waves similar to that associated with plasma expansion into vacuum also occurs in the transverse direction outside the beam. Because of electron trapping in the beam direction and the interactions between the trapped electrons and the electric field, the electron distribution is highly non-Maxwellian along the beam direction. Hence, the commonly used Boltzmann assumption for electron density in spacecraft plasma interaction models in general is not valid for interactions concerning plasma beam emission.

This paper and a companion paper [11] present an ongoing experimental and modeling investigation on ion beam neutralization. This paper further extends the modeling study of Wang and Usui [10] and addresses two aspects that were not studied previously. First, Wang and Usui [10] focused on the interaction process along the beam propagation direction. Here, we further exam the process in transverse direction and study whether the beam operating parameters, in particular the beam density/radius, would have any effects on ion beam neutralization. Second, Wang and Usui [10] focused on the in-space situation of beam emission. Here, we further include the effects of an imposed boundary condition and study whether the vacuum chamber wall would have any influence on ground experiments of beam neutralization. Additionally, this modeling study will also provide modeling predictions for the ongoing experimental study [11].

KINETIC SIMULATION MODEL

The ion beam neutralization process involves the following aspects: initial mixing of electrons and ions, electron-ion coupling, and beam propagation. The initial electron-ion mixing, to a large extent, is determined by device design and hence, the mixing process varies for different systems. In this paper, we will focus on the electron-ion coupling and beam propagation aspects.

The simulation model utilizes the electrostatic full Particle-In-Cell (PIC) method [12]. In this model, both the electrons and ions are modeled as macro-particles. The basic function of an electrostatic PIC code is to solve the electric field self-consistently with boundary conditions and the space charge of the particles from Poisson's equation, i.e.,

$$\nabla \cdot (\varepsilon_0 \vec{\nabla} \Phi) = e(n_e - n_i) \tag{1}$$

and the trajectories of each charged particle from Newton's second law, i.e.,

$$\frac{d}{dt}(m\vec{v}) = \vec{F} = q\vec{E},\ \vec{v} = \frac{d\vec{x}}{dt}. \tag{2}$$

The code used for this simulation study is a parallel immersed finite element (IFE) PIC code [13]. This code was used in various electric propulsion simulations, including several previous studies of ion beam neutralization [9, 10]. The parallel implementation of PIC is carried out through the merger of the University of California, Los Angeles Parallel PIC framework and the PIC subroutines written specifically for the applications. A detailed description of this Parallel IFE-PIC algorithm could be found in [13].

In order to reduce the computation, the 3-D PIC code is applied to a 2-D configuration ($x-z$) with a few cells in the third dimension (y) to maintain a symmetric boundary condition. The electrons and ions are emitted from the same surface area but with different velocity distribution functions. At every time step, macro-particles representing the ions are emitted into the simulation domain as a drifting Maxwellian distribution and those representing the electrons as a stationary Maxwellian distribution. In order to maintain the realistic relative velocity ratio between the beam velocity, and electron and ion thermal velocities in the simulation, the simulations are performed using the mass ratio of proton to electron, $m_i/m_e = 1836$. Comparing to the electron thermal velocity v_{te}, the ion drifting velocity v_{beam} and thermal velocity v_{ti} are $v_{beam} = 0.1v_{te}$ and $v_{ti} = 0.0023v_{te}$, respectively. These relative values are similar to typical ion thruster parameters. The emitted electron and ion currents are kept the same. For cold beam ions and thermal electrons, the electron and ion current density at the emitting surface are $J_{eo} = n_{eo} < v_{te} >$ and $J_{io} = n_{io}v_{beam}$, respectively. For the v_{te} and v_{beam} considered here, $n_{eo} = 0.25n_{io}$.

Typical domain size parameters of ground vacuum chamber are used as the benchmark case. The cell size equals the Debye length calculated using n_{io} and T_e at the emitting surface. We consider a spacecraft thruster with height (z) 2 and radius (x) 30. The beam emission radius is $R_b = 20$. The simulation domain is taken to be 128×80, or $6.4R_b \times 4R_b$. The potential at spacecraft body is fixed at zero. While the potential at domain boundary is floating, the gradient of

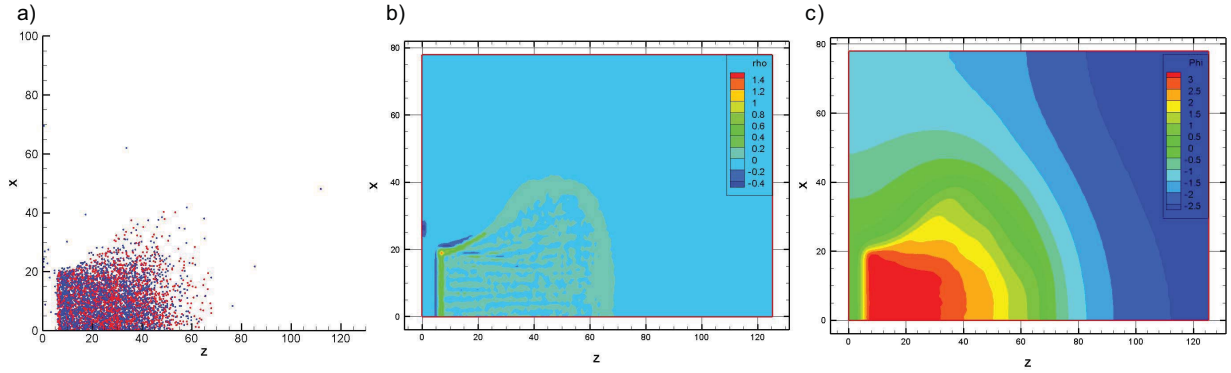

FIGURE 1. Benchmark case at $t\omega_{pe} = 400$: a) Electron (blue) and ion (red) positions. b) Total charge density contour. c) Potential contour.

it is set to zero (Neumann condition). The particle boundary condition is set to particle injection by calculating how many macroparticles are out of domain every time step. At the end of run, the total number of macroparticles used is typically around 10 million. Simulations use a time step resolution of $dt\omega_{pe} = 0.1$, and are run till $t\omega_{pe} = 400$.

RESULTS AND DISCUSSION

A number of simulations of ion beam neutralization have been performed. First, a benchmark case is presented to illustrate electron-ion coupling and the resulting propagation of the mesothermal plasma. Then, to examine the process in transverse direction and study whether the size of beam radius has any effects on ion beam neutralization, parametric simulations using different beam radius/Debye length are also discussed. Finally, to study the effects of an imposed boundary condition (from vacuum chamber wall or simulation domain), simulations using different boundary conditions and different simulation domain sizes are also discussed.

The Benchmark Case

Typical simulation results for a neutralized beam are presented in Fig. 1 through 2. Figure 1 shows electron and ion positions, total charge density contour and potential contour at $t\omega_{pe} = 400$. These results show that, while the beam is strongly nonneutral near the emitting source, the electron-ion coupling occurs immediately downstream of the emitting source and a quasi-neutral plasma beam quickly forms. The thermal electrons follow the motion of the cold beam ions, and the electron density closely matches the ion density inside the beam. For this particular case, the potential inside the beam downstream of the beam exit surface is only a few Te.

To investigate the process of electron and ion coupling, Figure 2 illustrates the phase plots, potential profiles, and the electron and ion charge density profiles along the beam direction at $t\omega_{pe} = 400$. (Animations showing the time evolution of these quantities are available in the conference presentation.) The initial electron expansion along the beam direction follows the same physical process studied in 1-D expansion of a mesothermal plasma into vacuum. It is well understood that such expansion establishes an ion-acoustic like beam front propagation. As the electron thermal velocity is much larger than the ion beam velocity, the region behind the beam front will have a slightly positive potential with respect to the ambient. Hence, the region between the beam source and the beam front gradually traps the electrons. It is the interaction between the trapped electrons and the potential well that leads to electron-ion coupling and beam neutralization. Further frequency and wave number spectrum analysis (not shown here) also show that no plasma instabilities were present. We find that ion beam neutralization is not through plasma micro-instability as previous studies suggested. As the beam front propagates forward, the electrons and ions develop a similar density profile along the beam direction, as shown in Fig. 2(c).

Once the quasi-neutral beam is established, an expansion wave is generated outside the beam shown in Fig. 1. The expansion in the transverse direction is similar to that associated with the self-similar expansion of a mesothermal plasma into vacuum.

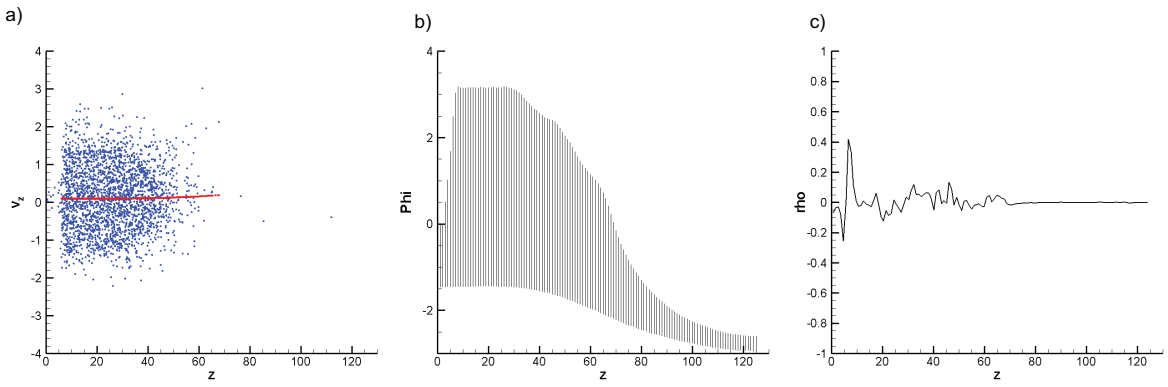

FIGURE 2. Benchmark case at $t\omega_{pe} = 400$: a) Electron and ion phase plot. b) Potential profile along the beam direction. c) Total charge density profile along the center axis.

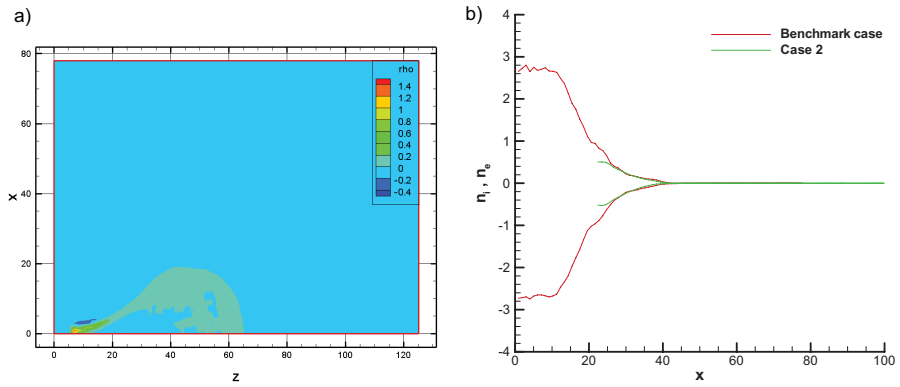

FIGURE 3. Case 2 at $t\omega_{pe} = 400$: a) Total charge density contour. b) Line-cut comparison of electron and ion density profile with benchmark case at $z = 40$.

Discussions

Effects of Beam Radius

To understand the physical process in transverse direction, a series of simulations with different beam radius/Debye length are performed to investigate whether the size of beam has any effects on the neutralization process. The smallest beam radius we used is 2 Debye length, and the results are shown below (case 2).

The total charge density contour and the comparison of electron and ion density profile with benchmark case at $z = 40$ are shown in Fig. 3. From the charge density contour, one could easily notice that the small radius beam is also neutralized and the expansion process in transverse direction is very similar to the benchmark large radius beam case, not only qualitatively, but also quantitatively in the size of expansion fan (around 20 Debye length). In Fig. 3(b), we shift the density profile of small radius case to make two profiles centered at same beam edge. It is clear that although the length of the core region is different due to different beam radius, the expansion profiles match nicely regardless of the beam radius. It indicates that the driving mechanism for the beam neutralization is still the electron-potential well collision along the beam propagating direction. And in the transverse direction, the physical process is just plasma expansion into vacuum. Figure 4 shows the potential contour and the comparison of potential profile with benchmark case. Again, we shift the potential profile of small radius case to match the beam edge with benchmark case in Fig. 4(b). In the beam expansion fan region, both potential profiles match closely. However, outside the expansion fan, the potential profiles tend to be different. This might be due to the difference of the beam radius and thus the difference of the length between the beam and the boundary.

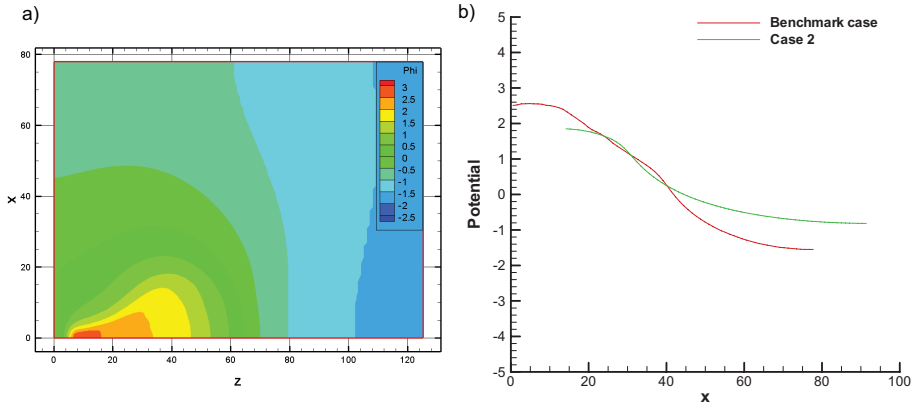

FIGURE 4. Case 2 at $t\omega_{pe} = 400$: a) Potential contour. b) Line-cut comparison of potential profile with benchmark case at $z = 40$.

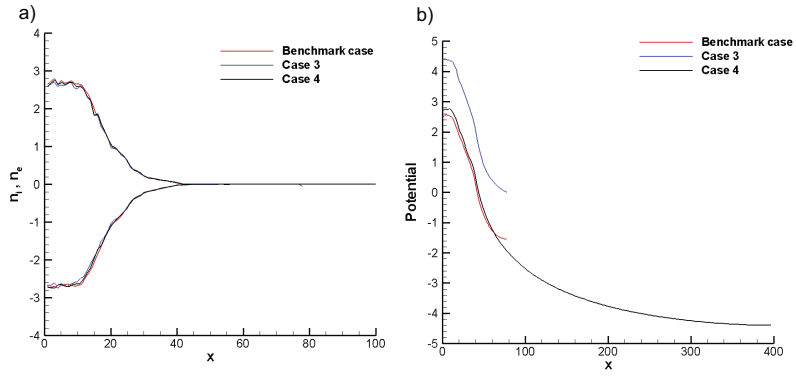

FIGURE 5. Case 3 and Case 4 at $t\omega_{pe} = 400$: a) Line-cut comparison of electron and ion density profile with benchmark case at $z = 40$. b) Line-cut comparison of potential profile with benchmark case at $z = 40$.

Effects of Boundary Condition

One of the major differences between ground test and in-space condition is that the potential of spacecraft is floating in space. To investigate whether the "floating potential" situation may be reproduced in a "fixed potential" environment, we change our field boundary condition to Dirichlet condition in case 3. Here, the potential is set to be zero at the boundary in stead of floating as in the benchmark case. The comparison of electron and ion density profile with benchmark case are shown in Fig. 5(a), and the comparison of potential profile with benchmark case are shown in Fig. 5(b). As shown in Fig. 5(a), the ion beam is fully neutralized with Dirichlet boundary condition. The density profile shows that it matches with benchmark case closely. In Fig. 5(b), we could notice that because we set the boundary potential to be zero, the potential inside the beam become larger than that of the benchmark case. However, the potential difference between the core beam and the boundary remains same as that of the benchmark case. By estimating the height of the curve in Fig. 5(b), the potential difference in both cases are around $4.4eV$. The above simulation results suggest that the difference between the Neumann and Dirichlet boundary condition is not significant for the same domain size.

Effects of Finite Domain Size

Another major difference between ground test and in-space condition is that ground tests are performed in a finite space. To study the effect of finite domain size, we perform a series of simulation cases with different domain size

while keeping other parameters the same as the benchmark case. The results (case 4) shown here have a domain size of 512×400 in Debye length, and our series of simulations shows that at such big simulation domain, the effect of domain size is minimized and the Neumann boundary condition is fully valid. Figure 5(a) shows the comparison of electron and ion density profile with the benchmark case and case 3. The comparison of potential profile are also shown in Fig. 5(b). As expected, in larger domain size case, the beam is fully neutralized, and density profile matches closely with benchmark case and case 3. The potential profiles inside the core beam and expansion fan region are also very close between larger domain and smaller domain case. However, outside the plasma expansion fan region, the larger domain tends to have a more negative potential profile along the transverse direction, which makes the potential difference from core beam to the boundary 65% larger than that of the benchmark case and case 3. Therefore, under ground vacuum chamber condition, our simulation results shows that the experiment could reproduce the ion beam neutralization process qualitatively. However, the expansion process outside of the beam would be affected significantly due to the limits imposed on the expansion process by the chamber wall. Therefore, the finite vacuum chamber size will affect measurements of quantitative parameters such as the beam potential

CONCLUSIONS

In summary, full particle PIC simulations are performed to study the ion beam neutralization process. Simulations further confirmed previous results from Wang and Usui [10]. We find that beam neutralization and propagation are two closely coupled processes. The initial expansion of thermal electrons over cold beam ions establishes ion-acoustic-like beam front propagation. Subsequently, the emitted electrons are trapped in the region between the forward propagating beam front and the emitting source. Electron-ion coupling is achieved through the interactions between the trapped electrons and the potential well along the beam direction. Beam neutralization is not through plasma instabilities as previous studies suggested. In the transverse direction outside the beam, the process is similar to that associated with plasma expansion into vacuum.

Our simulation also suggest that the finite size of experimental facilities may have a significant impact on the quantitative results of ion beam measured in ground tests. While the qualitative behavior of beam may be reproduced in a ground facility, quantitative parameters such as the beam potential cannot be predicted accurately due to the limits imposed on the expansion process by the finite chamber space.

ACKNOWLEDGMENTS

We acknowledge useful discussions with Drs. Yong Cao, Xiaoming He and Hide Usui.

REFERENCES

1. J. Wang, and S. Lai, *J. of Spacecraft Rockets* **34(6)**, 829–836 (1997).
2. O. Buneman, and G. Kooyers, *AIAA J.* **1(11)**, 2525–2528 (1963).
3. R. Wadhwa, O. Buneman, and D. Brauch, *AIAA J.* **3(6)**, 1076–1081 (1965).
4. D. Dunn, and T. Ho, *AIAA Preprint 63041* (1965).
5. H. Derfler, *Physics of Fluids* **7(10)**, 1625–1637 (1964).
6. O. Buneman, *J. Nucl. Energy C* **V2**, 119–134 (1961).
7. A. Wheelock, D. Cooke, and N. Gatsonis, *AIAA J.* p. 5148 (2003).
8. L. Brieda, and J. Wang, *AIAA J.* p. 4045 (2005).
9. Y. Cao, and J. Wang, *IEPC* p. 241 (2007).
10. J. Wang, and H. Usui, *IEPC* p. 263 (2009).
11. N. Ding, J. Polansky, J. Wang, and R. Downey, *Proceedings of 27th International Symposium on Rarefied Gas Dynamics, 174* (2010).
12. C. K. Birdsall, and A. B. Langdon, *Plasma Physics via Computer Simulation (Institue of Physics Publishing*, Institue of Physics Publishing, 1991.
13. J. Wang, Y. Cao, R. Kafafy, J. Pierru, and V. K. Decyk, *IEEE Transactions on Plasma Science* **34**, 2148–2158 (2006).